Phytochemistry Letters 17 (2016) 28–35

Contents lists available at ScienceDirect

Phytochemistry Letters

journal homepage: www.elsevier.com/locate/phytol

Alkaloidal metabolites from Aspergillus felis and their activities against Paracoccidioides brasiliensis

Graziele Mendes[a], Djalma de Menezes Oliveira[b], Markus Kohlhoff[c], Carlos Augusto Rosa[a], Tânia Maria de Almeida Alves[c], Carlos Leomar Zani[c], Luiz Henrique Rosa[a], Susana Johann[a], Betania Barros Cota[c,*]

[a] Department of Microbiology, Institute of Biological Sciences, Federal University of Minas Gerais, Presidente Antônio Carlos Avenue, 6627, Pampulha, 31270-901, Belo Horizonte, Minas Gerais, Brazil
[b] Department of Chemistry, State University of Bahia Southwest, José Moreira Sobrinho Avenue, 45206-191, Jequié, Bahia, Brazil
[c] Laboratory of Chemistry Bioactive Natural Products, René Rachou Research Center, Oswaldo Cruz Foundation, Augusto de Lima Avenue, 1715, Barro Preto, 30190-002, Belo Horizonte, Minas Gerais, Brazil

ARTICLE INFO

Article history:
Received 3 March 2016
Received in revised form 15 May 2016
Accepted 9 June 2016
Available online 28 June 2016

Keywords:
Aspergillus felis
Alkaloidal metabolites
Perhydroisoindol
Paracoccidioides brasiliensis
Antifungal activity

ABSTRACT

In this study, the fungus Aspergillus felis (strain UFMGCB 8030) was isolated from rocks in the Atacama Desert, Chile. Its CH_2Cl_2 extract exhibited antifungal activity (MIC of 1.9 mg/mL) against Paracoccidioides brasiliensis (Pb18), which is the etiological agent for paracoccidioidomycosis. The crude extract was purified, and a new cytochalasin derivative, cytochalasin Z_{15E} (1), and one ardeemin derivative, 5-N-acetyl-8-b-isopropyl-ardeemin (4), in addition to five known secondary metabolites, rosellichalasin (2), cytochalasin E (3), gancidin (5), pseurotin A1 (6), and 2,4-dihydroxyacetophenone (7), were isolated. The structures of these compounds were confirmed by 1D and 2D NMR spectroscopy and HR-ESI–MS. Cytochalasin E was the most active compound with MIC an value of 3.6 mM, while the other isolated compounds exhibited weak antifungal activities (MIC values >100.0 mM).

1. Introduction

The driest region in the world is the hyperarid Atacama Desert, Chile, where non-symbiotic fungi are widely distributed (Sterflinger et al., 2012). During our ongoing investigation toward the isolation of bioactive metabolites from fungi found in underexplored environments, we focused our attention on the Aspergillus felis strain UFMGCB 8030 isolated from the rocks of the Atacama Desert in northern Chile. The organic extract from this strain exhibited outstanding antifungal activity (MIC of 1.9 mg/mL) against the pathogenic fungus Paracoccidioides brasiliensis. P. brasiliensis causes paracoccidioidomycosis in humans, one of the most prevalent systemic mycoses in Latin America; it is a persistent infection that often develops after a long period of latency and cannot be easily eradicated with antifungal drugs (Bocca et al., 2013). Few research groups have explored natural products for finding drug leads aimed at finding alternative treatments or overcoming the issues that the drugs currently in clinical use cannot address. In this study, the isolation and structural determination of two new compounds, cytochalasin Z_{15E} (1) and 5-N-acetyl-8-b-isopropyl-ardeemin (4), along with the known compounds (2–3, 5–7) was reported. The isolated compounds were tested against the pathogenic fungus P. brasiliensis, and the results showed that cytochalasin E exhibits antifungal activity. In addition, secondary metabolites isolated from A. felis have been reported for the first time.

2. Results and discussion

The CH_2Cl_2 extract of A. felis was subjected to liquid–solid chromatography on a silica gel column to afford 12 fractions (F1–F12). Then, fractions F6 and F9 were subjected to RP18 semi-prep. HPLC to afford four (1, 4–6) and two alkaloidal metabolites (2–3) (Fig. 1), respectively. All known compounds were identified by the comparison of their spectral data (MS, and ^1H and ^{13}C NMR) with those published in literature.

Compound 1 was isolated as colorless oil with a specific rotation $[a]_D^{25}$ of +30.34 (c 0.78 in MeOH). The molecular formula was assigned as $C_{25}H_{33}NO_5$, as determined by HR-ESI–MS (m/z 428.2433, $[M+H]^+$; calc. for $C_{25}H_{34}NO_5$: 428.2431). Based on

* Corresponding author.
E-mail addresses: betania@cpqrr.fiocruz.br, bbcota9@gmail.com (B. Barros Cota)

http://dx.doi.org/10.1016/j.phytol.2016.06.006
1874-3900/

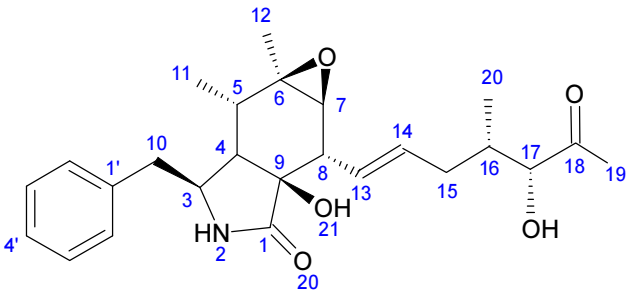

1

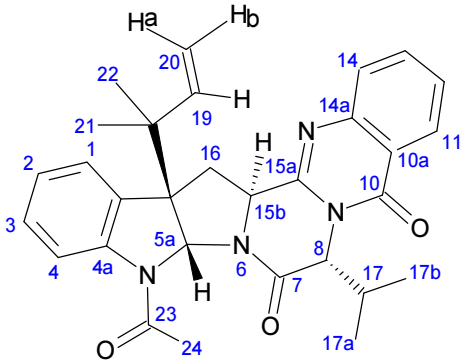

4

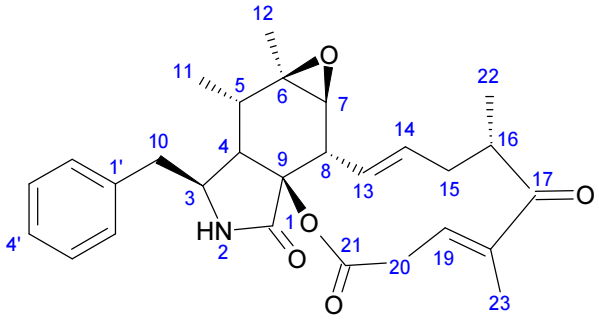

2

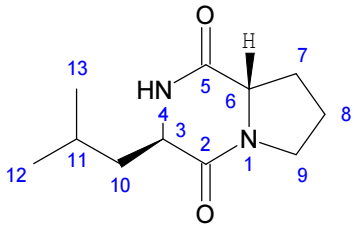

5

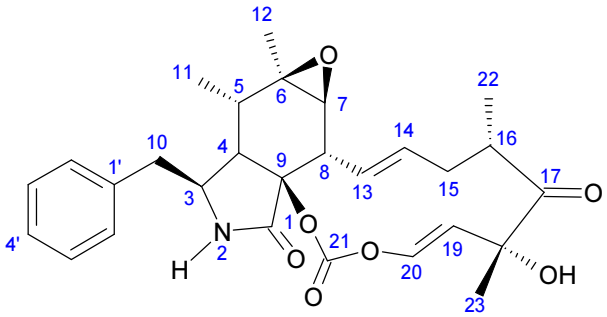

3

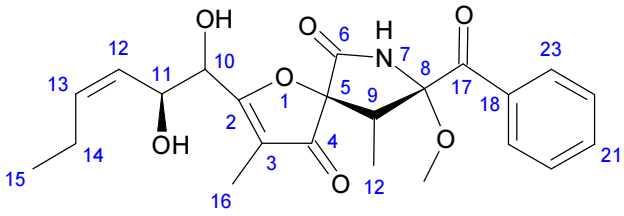

6

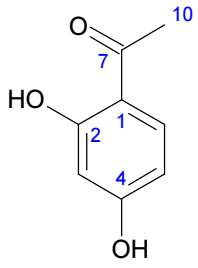

7

Fig. 1. Structures of compounds 1–7 isolated from Aspergillus felis.

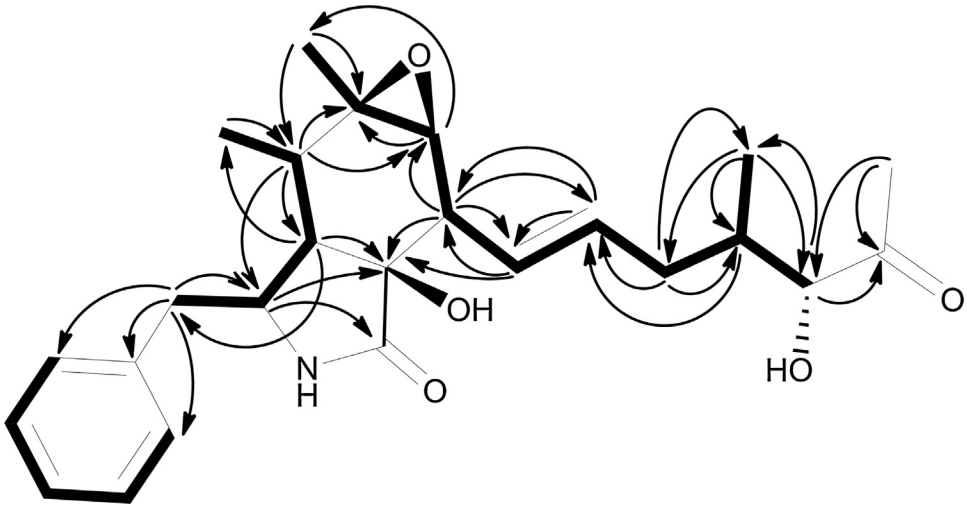

Fig. 2. Structure, key HMBC (!) and ^{1}H–^{1}H COSY (—) correlations of the cytochalasin Z_{15E} (1).

the molecular formula, it was deduced that 1 has 10 of unsaturation. Its UV spectrum exhibited λ_{max} at 204 and 256 nm. The ^{1}H, ^{13}C NMR, and HSQC data of 1 revealed two carbonyl and three non-hydrogenated carbons, as well as fourteen methine, two methylene, and four methyl groups. In the ^{1}H NMR spectrum of 1, aromatic signals were observed at a δ_H of 7.33 (2H, dt, J=7.5, 1.8 Hz, H-3′/5′), δ_H 7.30–7.27 (1H, m, H-4′), and δ_H 7.19–7.16 (2H, m, H-2′/6′), indicative of a monosubstituted phenyl ring. The COSY spectrum showed correlations between aromatic protons, attributed to the presence of cross peaks between H-2′/6′and H-3′/5′and H-3′/5′and H-4′. The correlations between H-2′/6′ and C-10 (δ_C 45.10, CH_2) indicated the presence of a benzyl moiety, which was attached at C-3 (δ_C 54.45, CH), attributed to the cross peak between H_2-10 (δ_H 2.98 and δ_H 2.69) and C-3 in the HMBC spectrum (Fig. 2). In the ^{1}H NMR spectrum of 1 (Table 1), a signal corresponding to amide NH (δ_H 6.19) was observed, and in the ^{13}C NMR spectrum, two carbonyl carbon signals were observed at δ_C of 210.5 and 175.5, attributed to ketone and amide carbons, respectively. The 1D and 2D NMR spectra of 1 also showed peaks corresponding to a 10-phenylsubstituted perhydroisoindol-1-one skeleton with a 6,7-epoxy moiety, as well as spectral data very similar to the known series of cytochalasins, mainly with the cytochalasins Z_{20} and Z_{21} (Wang et al., 2011; Lin et al., 2009; Liu et al., 2006, 2008). The chemical shifts of C-6 and C-7 in 1 observed at δ_C 59.9 (C) and 61.5 (CH), respectively, were very similar to those recorded for cytochalasin Z_{20} (C-6: δ_C 60.5, C and C-7: δ_C 61.2, CH) (Lin et al., 2009) and Z_{21} (C-6: δ_C 59.3, C and C-7: δ_C 61.2, CH) (Wang et al., 2011). COSY correlations confirmed the perhydroisoindol-1-one skeleton with a 6,7-epoxy moiety by the presence of cross peaks between H-3 and H-4, H-4 and H-5, H-5 and H-11, and H-7 and H-8/H-12 (Fig. 2). The HMBC spectrum helped to confirm this individual fragment by correlations between H-10 and C-1′/C-3/C-

Table 1
NMR spectroscopic data for cytochalasin Z_{15E} (1) (at 400 MHz for ^{1}H and 100 MHz for ^{13}C).

Position	1 in $CDCl_3$			
	δ_C, type	δ_H (J in Hz)	COSY	HMBC[a]
1	175.5, C			
2	N H	6.19, br. s.		
3	54.5, CH	3.63, dt (9.0, 4.5)	4, 10a, 10b	1, 4, 5, 9, 1′
4	50.5, CH	2.40, dd (8.0, 4.5)	3, 5	1, 3, 5, 6, 8, 9, 10, 11
5	33.9, CH	2.34, dd (8.0, 7.0)	4, 11	3, 4, 6, 7, 9, 11,12
6	59.9, C			
7	61.5, CH	2.97, br. d (5.0)	8, 12	6, 8, 9, 12, 13
8	48.8, CH	2.75, br. dd (8.0, 5.0)	7, 13, 14	1, 4, 6, 7, 9, 13, 14
9	77.9, C			
10	45.1, CH_2	a: 2.69, dd (13.0, 9.5)	3, 10b	3, 4, 1′, 2′/6′
		b: 3.04–2.93, m	3, 10a	3, 4, 1′, 2′/6′
11	14.2, CH_3	1.11, d (7.0)	5	4, 5, 6
12	21.1, CH_3	1.33, br. s	7	5, 6, 7
13	127.2, CH	5.75–5.69, m	8, 14, 15a, 15b	7, 8, 9, 14, 15
14	135.1, CH	5.74 ddd (15.5, 9.0, 6.8)	8, 13, 15a, 15b	8, 13
15	37.4, CH_2	a: 2.24–2.16, m	8, 14, 15b, 16	13, 14, 16, 17, 20
		b: 2.25, dddd (14.1, 7.0, 6.8, 1.7)	13, 14, 15a, 16	13, 14, 17, 20
16	36.0, CH	2.07, dtd (8.6, 6.8, 6.8, 2.0)	15a, 15b, 17, 20	14, 15, 20
17	78.6, CH	4.17, d (2.0)	16	15, 16, 18, 20
18	210.5, C			
19	25.7, CH_3	2.15, s		17, 18
20	13.0, CH_3	0.71, d (6.8)	16	15, 16, 17
1′	137.4, C			
2′/6′	129.2, CH	7.18–7.16, m	3′,5′	10, 3′/5′, 4′
3′/5′	129.2, CH	7.33, dt (7.5, 1.8)	2′, 6′	1′, 2′/6′
4′	127.4, CH	7.30–7.28, m	3′,5′	2′/6′

[a] HMBC correlations are from proton (s) stated to the indicated carbon.

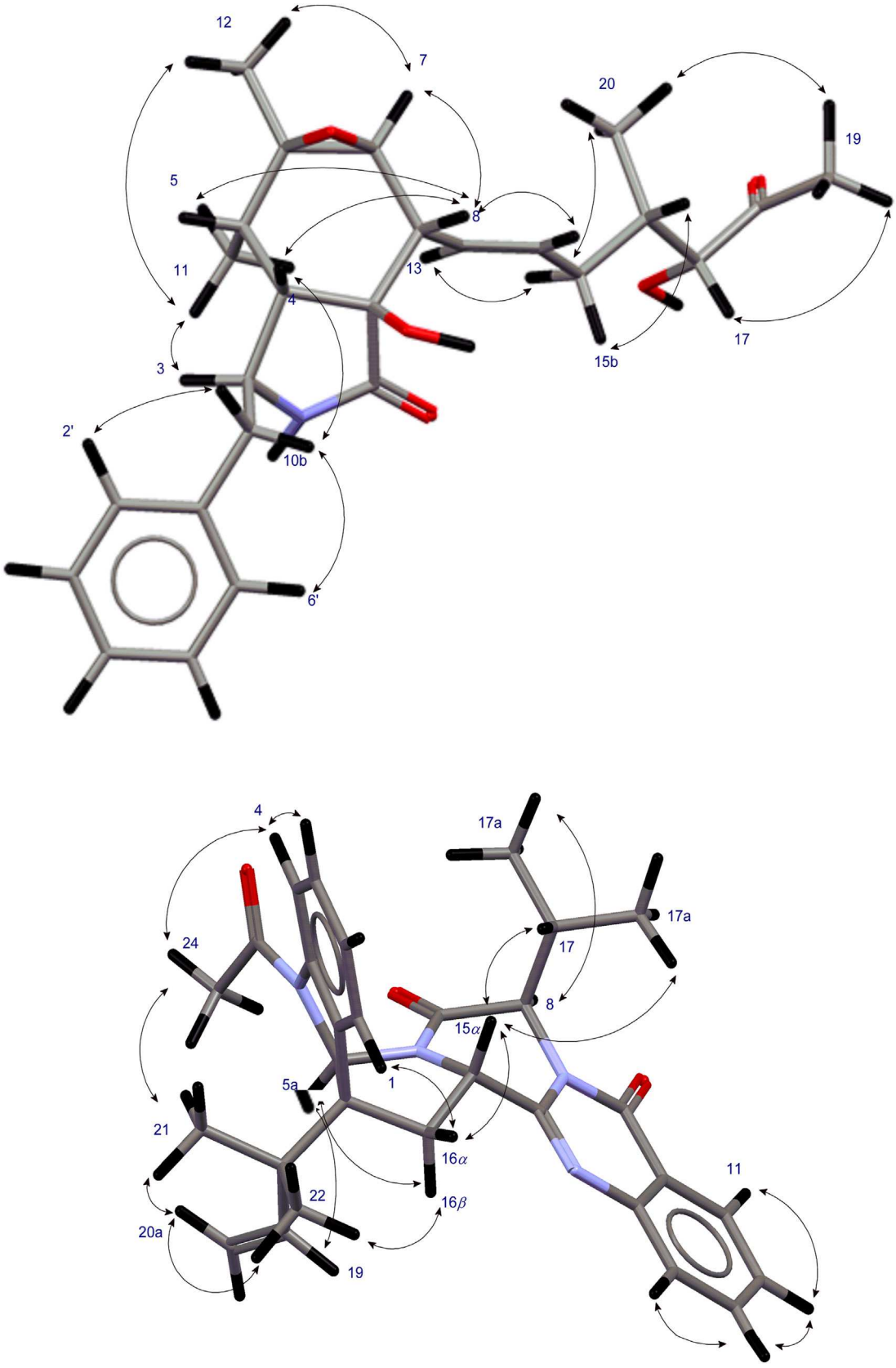

Fig. 3. Main NOESY correlations of the cytochalasin Z_{15E} (1) and 5-N-acetyl-8-b-isopropyl-ardeemin (4).

4, H-3 and C-1/C-4/C-5/C-9/C-1′; H-5 and C-3/C-4/C-6/C-11/C-12, H-7 and C-6/C-8/C-9/C-12, and H-8 and C-9/C-1 (Fig. 2). Comparison between the NMR data of compound 1 and those reported to Z_{21} showed R^2 values ($\alpha = 0.05$) very significant for both δ_C (0.999) and δ_H (0.998).

The ^{1}H NMR spectrum of 1 also showed signals at δ_H 5.74 and 5.73–5.69, attributed to a double bond. The double bond was confirmed by HSQC analysis, which showed two corresponding methine signals at δ_C 135.1 and 127.2, respectively. The ^{1}H NMR spectrum of 1 was analyzed using TopSpin 3.2 and PERCH NMR software, which enabled the recovery of information with respect to the spin coupling constants related to H-14, the signal of which was partially overlapped by that of H-13. The coupling constants measured between H-14 and H-13 (J = 15.5 Hz), H-15a (J = 9.0 Hz), H-15b (J = 6.8 Hz) allowed for the assignment of the signal at δ_H 5.74 (1H, ddd, J = 15.5, 9.0, 6.8 Hz, H-14). Thus, the geometry of the double bond between C-13 and C-14 is likely trans, attributed to the coupling constant value (J_{13-14} = 15.5 Hz) (Fig. 2). The NOESY correlations corroborate this assignment because the H-14 signal is correlated with H-7 and H-8 (Fig. 3), while the H-13/H-14 cross peak was not recorded.

Besides the 10-phenylsubstituted perhydroisoindol-1-one skeleton, the 1D and 2D NMR indicated that 1 has an open 8-carbon chain system rather than a macrocyclic ring (Fig. 1, Table 1). In the COSY spectrum, cross peaks were observed between H-8 and H-13/H-14, H-14 and H-15a, H-15a and H-14/H-15b, H-15b and H-13/H-14/H-16, and H-16 and H-17/H-20. This third spin system was also deduced by the HMBC spectrum (Fig. 2), confirmed by the correlation between H-13 and C-14, as well as the correlations of both H-15a and H-15b with C-13/C-14/C-17/C-20 and H-16 with C-14/C-15/C-20. In addition, in the HMBC contour map, correlations were observed between H-17 and C-15/C-16/C-18/C-20; finally, H-19 exhibited cross peaks with C-17 and C-18. On the other hand, the comparison of the 1D NMR spectra of 1 with that of cytochalasin Z_{20} (Lin et al., 2009) indicated that these compounds are very similar, except for the position of the carbonyl and hydroxyl in the 8-carbon chain system. The main differences in the ^{13}C NMR of 1 were observed at C-16 to C-20 (C-16: δ_C 36.0; C-17: δ_C 78.6; C-18: δ_C 210.5; C-19: δ_C 25.7; and C-20: δ_C 13.0) (Table 1). The chemical shifts of C-17 (δ_C 78.6) and CH_3-20 (δ_C 13.0) in 1 were downfield and upfield, respectively, considering the same carbons at cytochalasin Z_{20} (C-17:δ_C 73.2 and CH_3-20: δ_C 17.2) (Lin et al., 2009).

The magnitude of the coupling constant corresponding to the signal at δ_H 2.75 ($J_{8,7}$ = 5.0 Hz, H-8) reveal that H-8 and H-7 have dihedral angles of approximately 53°, indicating α-equatorial and β-axial location of H-7 and H-8, respectively (Smith and Barfield, 1993). The relative configuration of the stereocenters in the isoindolone moiety of 1 was deduced from the NOESY correlations of H-5 and H-8 and between H-4 and H-8, which indicated that H-4, H-5, and H-8 are on the same face of the molecule and assigned to have β-orientation. In addition, all cytochalasins isolated thus far have the same configuration of cyclohexane and isoindole moieties (Lin et al., 2009). Therefore, the 1D and 2D NMR data comparison, the results of NOESY analysis and the biogenetic origin allowed to assign the same relative configuration previously found in Z_{20} and Z_{21} to the epoxyperhydroisoindol 6,7-1-1-one moiety of 1.

The relative configurations of the stereogenic centers at C-16 and C-17 in the open 8-carbon chain in 1 were proposed on the basis of the correlations between H-17 (δ_H 4.17) and H-16 (δ_H 2.07) and H-15b (δ_H 2.25) in the NOESY spectrum, indicative of an anti relationship between H-17 and H-20. This assumption was confirmed by the HMBC correlation of a δ_H of 2.07 and a δ_C of 13.0 ($^3J_{C\text{-}20,\ H\text{-}17}$), as well as the non-detection of cross peak of the coupling constant $^2J_{C\text{-}17,\ H\text{-}16}$, suggesting that H-16 and the hydroxyl at C-17 are in anti arrangement. Furthermore, the absence of correlation between H-17 (δ_H 4.17) and H-20 (δ_H 0.71) confirmed this relative orientation, and the peak between CH_3-20 (δ_H 0.71) and H-15a (δ_H 2.16–2.24) in the NOESY spectrum indicated that these two protons are on the same side.

In addition, the relative stereochemistry of the fragment between C-15 and C-18 of 1 was assigned on the basis of the homonuclear and heteronuclear coupling constant values obtained by HMBC and ^{1}H NMR spectral analysis. The molecular modeling system (MMS) of PERCH was utilized for the molecular modeling of 1, and the ^{13}C and ^{1}H NMR spectra were predicted using PERCH-NMR software. Table 2 shows the experimental and estimated values of the coupling constants $^{2,3}J_{C,H}$ and $^3J_{H,H}$ for the 1-methyl-2-hydroxy system relative to C-16/C-17, which were calculated using the measurement and estimation from ^{1}H NMR spectra and phase-sensitive HMBC. The data indicated that the fragment exhibits a majority of the threo-1,2-methyl-hydroxyl configuration (Matsumori et al., 1999; Bifulco et al., 2007). Thus, the configuration of the stereogenic centers at C-16 and C-17 is presumed to be S and R, respectively, according to open-chain cytochalasins Z_{15} (Liu et al., 2008), and on the basis of biogenetic origin, all cytochalasins isolated thus far have the same absolute configuration in the 10-phenylsubstituted perhydroisoindol-1-one skeleton and at C-16 of the macrocyclic ring moieties (Lin et al., 2009; Liu et al., 2008). Thus, the structure of 1 is tentatively established as (13E)-(3S,4S,5S,6R,7S,16R,17R)-6,7-epoxy-16-methyl-17-hydroxy-10-phenyl-[14]cytochalasa-13-ene-1,18-dione, namely cytochalasin Z_{15E}.

Compound 4 was isolated as a colorless amorphous solid. Its UV spectrum exhibited λ_{max} at 206, 228, 270, and 305 nm. The molecular formula was $C_{30}H_{32}N_4O_3$, as determined by HR-ESI–MS (m/z 497.2553, $[M+H]^+$; calc. for $C_{30}H_{33}N_4O_3$: 497.2547). The COSY experiment indicated the presence of two aromatic spin systems with coupled protons at δ_H of 7.92 (H-4), 7.54 (H-1), 7.37 (H-3), and 7.26 (H-2), and another one at a δ_H of 8.20 (H-11), 7.83 (H-13), 7.71 (H-14), and 7.52 (H-12). 1D and 2D NMR analysis of 4 indicated that it has a structure similar to that of ardeemin derivatives (Hochlowski et al., 1993). The molecular formula was assigned as $C_{30}H_{32}N_4O_3$, implying 17 of unsaturation. The unsaturations were accommodated such as 5-N-acetylardeemin: eight in the two substituted benzene rings, two in carbonyl functions, one in the olefin of the isoprenoid unit, one in amidine function, and four in the other four rings (Hochlowski et al., 1993). The only difference was the presence of an isopropyl moiety (δ_C 32.6/δ_H 1.97, C-17/CH;

Table 2
Estimated and calculated $^{2,3}J_{C,H}$ e $^3J_{H,H}$ values for the C16-C17 segment in 1.

$^{2,3}J_{XH}$	Estimated (Hz)[b]	Calculated (Hz)[c]	Magnitude[d]
$^3J_{H\text{-}16,H\text{-}17}$	1.8	1.3	Small
$^3J_{C\text{-}15,H\text{-}17}$	3.9	1.4	Medium
$^3J_{C\text{-}18,H\text{-}16}$	1.0	1.2	Small
$^3J_{C\text{-}20,H\text{-}17}$	6.4	7.2	Large
$^2J_{C\text{-}17,H\text{-}16}$	< 0.5	0.5[a]	Small

[a] Empirical value based on the non-detected correlation $^2J_{C17,H16}$ in the HMBC spectrum. Experimentally, this value ranges from 0 to 2 Hz.

[b] $^3J_{H,H}$ values were extracted from the ^{1}H NMR spectrum. The $^{2,3}J_{C,H}$ values were estimated by the PS-HMBC spectrum through the rationalization of the relative intensities of the cross peaks by the equation $I_{Ca,H}/I_{Cb,H} \approx \sin^2(\Delta\pi J_{Ca,H}) / \sin^2(\Delta\pi J_{Cb,H})$, where $I_{Ca,H}$ and $I_{Cb,H}$ are the cross peak intensity, attributed to H-Ca and H-Cb couplings, respectively, whereas Δ represents the delay of long-range proton-carbon coupling evolution of the HMBC experiment.

[c] Values calculated by Karplus-type equations. The dihedral angles of 1 were calculated by a molecular modeling system (MMS) with 3D molecular models having energetic optimization by Merck molecular force field (MMFF94).

[d] Systems 1-methyl-2-hydroxy, the magnitude of coupling constant values, in Hz, are estimated as follows: Small = [(1 < $^3J_{H,H}$ < 4), (1 < $^3J_{C,H}$ < 3), (0 < $^2J_{C,H}$ < 2)]; large = [(8 < $^3J_{H,H}$ < 11), (6 < $^3J_{C,H}$ < 8), (5 < $^2J_{C,H}$ < 7)].

δ_C 20.3/δ_H 0.88; C-17b/CH_3; and δ_C 18.9/δ_H 0.85, C-17a/CH_3) in 4 instead of a methyl group in position 8, as previously reported for 5-N-acetylardeemin (Zhang et al., 2014; Zhang et al., 2010; Hochlowski et al., 1993). Furthermore, the HMBC experiment indicated cross peaks between δ_H 5.10 (H-8) and δ_C 32.6 (C-17), δ_C 18.9 (C-17a), and δ_C 20.3 (C-17b), which permitted the confirmation of this connectivity. Based on NOESY correlations (δ_H 5.10, H-8 and δ_H 1.97, H-17) (Fig. 3, Table 3) and the coupling constant of vicinal protons J_{8-17} (8.4 Hz), 4 was elucidated as (7R,9aS,14bR,15aR)-10-acetyl-10,14b,15,15a-tetrahydro-7-isopropyl-14b-(2-methylbut-3-en-2 yl)indolo[3″,2″:4′,5′]pyrrolo [2′,1′:3,4]pyrazino[2,1-b]quinazoline-5,8(7H,9aH)-dione, namely 5-N-acetyl-8-b-isopropyl-ardeemin.

The crude CH_2Cl_2 extract from A. felis exhibited an MIC value of 1.9 mg/mL against P. brasiliensis. All isolated compounds were tested by the same assay for evaluating their antifungal activities. Cytochalasin E exhibited the highest activity with an MIC of 1.8 mg/mL (3.6 mM), followed by 4 (MIC=62.5 mg/mL=125.9 mM), 2 (MIC=62.5 mg/mL=134.8 mM), and 6 (MIC=62.5 mg/mL=144.9 mM) (Table 4). Cytochalasin E and rosellichalasin have been both isolated from Rosellinia necatrix (Kimura et al., 1989), Aspergillus flavipes (Lin et al., 2009), Aspergillus terreus (Ge et al., 2010; Zhang et al., 2010), Aspergillus sp. nov. F1 (Xiao et al., 2013), and Xylaria sp. (Zhang et al., 2015); their structures primarily differ in the side chains at carbons 18–21. According to Xiao et al. (2013), both cytochalasin E and rosellichalasin exhibit cytotoxic activity against A549, Hela, BEL7402, and RKO cells with IC_{50} values varying from 37.3–78.5 mM. However, only cytochalasin E exhibits activity against HepG2 and CaSki cancer cells with IC_{50} values of 25 mM and 29 mM, respectively (Zhang et al., 2015).

In our assays, only cytochalasin E exhibited outstanding antifungal activity against P. brasiliensis. Cytochalasin E has been previously reported to be the antifungal component in Xylaria sp. XC-16, exhibiting activity against Alternaria solani (MIC of 50 mM), Botrytis cinerea, and Gibberella saubinetti (MICs of 100 mM) (Zhang et al., 2014).

3. Experimental

3.1. General

UV spectra were measured on a SpectraMax® M5 multi-mode microplate reader (Molecular Devices, California, USA). Optical rotation was recorded using an Anton Paar MCP 300 polarimeter. 1D and 2D NMR spectra were recorded on a Bruker Avance 400 MHz spectrometer using TMS as the internal standard. High-resolution mass spectra were recorded on a Bruker ETD-maXis quadrupole TOF (Bruker Daltonics, Bremen, Germany) coupled to a Thermo Surveyor Plus HPLC system (Thermo Fisher Scientific, Waltham, MA, USA) equipped with a Finnigan PDA Surveyor Plus diode-array detector. Analyses were conducted on a reverse-phase column (Atlantis C_{18}, Waters, USA, particle diameter of 3 mm, 150 mm × 2.1 mm i.d.) using a linear gradient of ACN:H_2O from 10 to 100% in 12.5 min. The following conditions were utilized: end plate offset, −500 V; capillary voltage, 4500 V; nebulizer pressure, 0.4 bar; dry gas (nitrogen) flow rate, 4.0 L/min; dry temperature, 180 °C; ISCID energy, 25 eV; collision energy, 7 eV; ion cooler RF, 25 Vpp; transfer time, 45–49 ms; and mass range, 50–1500 Da. Analytical HPLC was performed on a Shim-pack® C18 column (5 mm, 4.6 mm × 250 mm, i.d.) using a system (Shimadzu, Kyoto, Japan) equipped with an LC10AD pump and an SPD M-10A VP diode array detector. Semi-prep. purification was conducted using an HPLC system (Shimadzu, Kyoto, Japan) equipped with two LC6AD pumps and an SPD-10A-UV detector. TLC analyses were

Table 3
NMR spectroscopic data for 5-N-Acetyl-8-b-isopropyl-ardeemin (4) (at 400 MHz for ^1H and 100 MHz for ^{13}C).

	4 in CD_3OH			
Position	δ_C, type	δ_H (J in Hz)	COSY	HMBC[a]
1	126.4, CH	7.54, dd (8.0, 1.5)	2	3, 4, 4a, 16a
2	126.2, CH	7.26, td (7.5, 1.5)	1, 3	4, 4a
3	130.1, CH	7.37, td (7.5, 1.5)	2, 4	2, 4, 4a
4	120.3, CH	7.92, br. d (7.5)	3	
4a	144.0, C			
5a	80.9, N[illegible]H	6.13, br. s.		
7	166.8, C			
8	63.9, CH	5.10, d (8.4)	17	7, 10, 15a, 17, 17a, 17b
10	162.2, C			
10a	121.5, C			
11	127.8, CH	8.20, dd (8.5, 1.5)	12, 13	10, 12, 13, 14a
12	128.5, CH	7.52, dd (7.5, 1.5)	11, 13	10, 14a
13	136.1, CH	7.83, ddd (8.5, 7.0, 1.5)	12, 14	10a, 11, 14a
14	128.3, CH	7.71, br. d (8.5)	12, 13	10, 10a, 12, 14a
14a	148.6, C			
15a	153.0, C			
15b	60.2, CH	4.53, dd (10.5, 6.0)	16a, 16b	14a, 15a, 16
16	37.4, CH_2	b: 2.77, dd (13.0, 10.5)	15b, 16a	15a, 15a, 18
		a: 3.08, dd (13.0, 6.0)	15b, 16b	5a, 15b, 16b
16a	62.4, C			
16b	136.1, C			
17	32.6, CH	1.97, dquin (8.4, 6.8 × 4)	8, 17a	7, 8, 17a, 17b
17a	18.9, CH_3	0.85, d (6.8)	17	8, 17, 17b
17b	20.3, CH_3	0.88, d (6.8)		8, 17a
18	41.4, C			
19	144.9, CH	5.87, dd (17.4, 10.8)	20a	16a, 18, 22
20	114.7, CH_2	a: 5.14, br. d (17.4)	19, 20b	18, 19
		b: 5.08, d (10.8, 0.9)	20a	18, 19
21	22.8, CH_3	1.22, s	22	16a, 18, 19, 20, 22
22	23.8, CH_3	1.05, s	21	16a, 18, 19, 20, 21
23	172.5, C			
24	23.9, N[illegible]H	2.66, br. s.		23

[a] HMBC correlations are from proton (s) stated to the indicated carbon.

Table 4
MIC values of isolated compounds from Aspergillus felis against Paracoccidioides brasiliensis (Pb18) using microdiluition broth assay.

Sample	Pb 18 μg/ml
Crude extract	1.9
Cytochalasin Z_{15E} (1)	250.0
Rosellichalasin (2)	62.5
Cytochalasin E (3)	1.8
5-N-Acetyl-8-β-isopropyl-ardeemin (4)	62.5
Gancidin (5)	>250.0
Pseurotin A1 (6)	62.5
2,4-Dihydroxyacetophenone (7)	250.0
Itraconazol	0.001
Amphotericin	0.06

conducted on pre-coated silica gel G-60/F254 plates (0.25 mm, Merck, Darmstadt, Germany).

3.2. Isolation of fungal material

The fungus A. felis (UFMGCB 8030) was isolated from rocks collected from the Atacama Desert, Chile. It was preserved in sterile distilled water (Castellani, 1967) in the Collection of Microorganisms and Cells at the "Universidade Federal de Minas Gerais," Brazil.

3.3. Identification of fungus

The fungus UFMGCB 8030 was identified on the basis of the analysis of ITS, β-tubulin, and RPB2 gene regions. The nucleotide sequence of ITS of UFMGCB 8030 indicated 100% of query coverage and 100% similarity with a sequence of A. felis (GenBank code KF558318). In addition, β-tubulin sequences indicated 84% of query coverage and 99% similarity with a sequence of A. felis (GenBank code KJ914694), while RPB2 nucleotide sequences indicated 100% of query coverage and 98% similarity with the sequence of A. felis (GenBank code KJ914735). The fungus UFMGCB 8030 was identified as A. felis (Gonçalves et al., 2016; Mendes et al., 2016). The sequences were deposited in GenBank under accession codes KX098586 (ITS) and KX229737 (β-tubulin).

3.4. Fermentation and extraction

The fungus A. felis was grown under static conditions at 25 °C for 15 days in 600 Petri dishes (90 mm diameter) containing 20 mL of potato dextrose agar composed of dextrose (2%w/v), potato infusion (30%w/v), and agar (2%w/v). The culture was extracted two times with CH_2Cl_2 for 48 h. The suspension was filtered using filter paper, and the organic phases were concentrated on a rotary evaporator. The residual solvent was dried by vacuum centrifugation at 40 °C overnight, affording the CH_2Cl_2 extract (5.8 g).

3.5. Purification and isolation

Next, the CH_2Cl_2 extract (5.8 g) was subjected to column chromatography (CC) using a silica-gel (230–400 mesh) open column using a gradient of solvents with increasing polarity: Hex, Hex/CH_2Cl_2 (1:1, v/v), CH_2Cl_2, CH_2Cl_2:EtOAc (1:1–7:3, v/v), EtOAc, EtOAc/MeOH (1:1, v/v), and finally with MeOH, affording 12 fractions (F1–12). Fraction 6 (350 mg) was purified by semi-prep. RP-HPLC (220 and 254 nm, Shim-pack® C18, 5 mm, 20 × 250 mm, i.d., 7 mL/min) using a gradient of ACN in H_2O (10–100% over 50 min) followed by 100% ACN for 20 min, affording 1 (20 mg), 4 (6 mg), 5 (15 mg), and 6 (4 mg). Fraction 9 (162 mg) was subjected to semi-prep. RP-HPLC (220 and 254 nm, Shim-pack® C18, 5 mm, 20 × 250 mm, i.d., 7 mL/min) using a gradient of ACN in H_2O, 10–80% over 60 min, followed by 80–100% of ACN for 4 min, and 100% of ACN for 10 min, affording 2 (9 mg), 3, (11 mg), and 7 (8 mg).

3.5.1. Compound 1

Cytochalasin Z_{15E}, (13E)-(3S,4S,5S, 6R,7S,16R,17R)-6,7-epoxy-16-methyl-17-hydroxy-10-phenyl-[14]cytochalasa-13-ene-1,18-dione: 20 mg; colorless oil; $[\alpha]_D^{25}$ +30.34 (c 0.78, MeOH); UV (MeOH) λ_{max} (log ε) 204 (3.65), 256 (2.66); for ^1H and ^{13}C NMR spectroscopic data, see Table 1; HRMS m/z 428.2433, $[M+H]^+$ (calc. for $C_{25}H_{34}NO_5$: 428.2431).

3.5.2. Compound 4

5-N-acetyl-8-β-isopropyl-ardeemin, (7R,9aS,14bR,15aR)-10-acetyl-10,14b,15,15a-tetrahydro-7-isopropyl-14b-(2-methylbut-3-en-2-yl)indolo[3″,2″,4″,5″]pyrrolo[2′,1′,3,4]pyrazino[2,1-b]quinazoline-5,8(7H,9aH)-dione: 6 mg; colorless amorphous solid; $[\alpha]_D^{25}$ −31.67 (c 0.6, MeOH); UV (MeOH) λ_{max} (log ε) 206 (4.41), 228 (4.24), 270 (3.79), and 305 (3.42) nm; for ^1H and ^{13}C NMR spectroscopic data, see Table 3; HRMS m/z 497.2553, $[M+H]^+$ (calc. for $C_{30}H_{32}N_4O_3$: 497.2547).

3.6. Antifungal assay

The antifungal activity of the samples was evaluated against a P. brasiliensis (Pb18) isolate belonging to the phylogenetic species S1 by the broth microdilution susceptibility test. The Pb18 isolate was maintained by weekly transfer in solid YPD medium (peptone, yeast extract, and dextrose) at 37 °C. The isolated Pb18 cells were suspended in sterile saline, and the transmittance of the supernatant at 530 nm was adjusted to 70% (1 × 10^6 to 5 × 10^6 cells/mL). The cell suspension was diluted in 1:10 RPMI 1640 broth plus 3-(N-morpholino)propanesulfonic acid buffer to the final inoculum of 1 × 10^5 to 5 × 10^5 cells/mL (Cruz et al., 2012; Clinical Laboratory Standards Institute, 2008). Samples were diluted serially using RPMI 1640 broth at concentrations ranging from 500.0 to 0.9 μg/mL for obtaining minimal inhibitory concentrations (MICs). Itraconazol (0.5–0.0005 μg/mL) and amphotericin (0.5–0.0005 μg/mL) were used as positive controls. MIC, expressed in μg/mL, was defined as the lowest concentration at which 100% inhibition of the growth of isolated Pb 18 could be achieved. Results were obtained in three independent experiments performed in duplicate.

3.7. Computational simulations

The intensities of the long-distance correlations $^{2,3}J_{H,C}$ and $^3J_{HH}$ were measured by a spectrum obtained by a standard experiment, obtained from a program hmbcetgpl3nd pulses (Cicero et al., 2001), using a BRUKER spectrometer of 400 MHz. $CDCl_3$ was used as the solvent. Phase-sensitive HMBC using an echo/antiecho gradient selection was used with a three-fold low-pass J-filter for suppressing one-bond correlations as well as decoupling during acquisition. This experiment was processed to obtain a phase-sensitive ^1H–^{13}C long-range correlation spectrum (PS-HMBC) using TOPSPIN software (version 3.2). This pulse program was chosen because the echo-anti-echo detection mode results in high sensitivity, in addition to the 3rd order low-pass filter, which is more efficient at eliminating ^1J artifacts. The J values in this parameter set were selected for optimizing ^2J-^3J correlations. HMBC experiments were recorded at frequencies of 400.15 MHz (^1H) and 100.62 (^{13}C) with a delay Δ set at 62.5 ms with a size date of 2048 (F2) × 256 (F1) points, total number of scans set at 16, spectral widths of 3422.99 Hz (^1H) and 22299.63 Hz (^{13}C), and the spectral resolution of 1.672196 (F2) and 21.798269 (F1). The data were processed using sine (t_2) and a sine-bell squared (t_1) window functions.

Acknowledgments

We acknowledge the "Conselho Nacional de Desenvolvimento Científico e Tecnológico" (CNPq) for financial support and scholarship. This study was also supported by the Program of Technological Development in Tools for Health-PDTIS-FIOCRUZ analytical platform (RPT13A) for NMR experiments.

Appendix A. Supplementary data

Supplementary data associated with this article can be found, in the online version, at http://dx.doi.org/10.1016/j.phytol.2016.06.006.

References

Bifulco, G., Dambruoso, P., Gomez-Paloma, L., Riccio, R., 2007. Determination of relative configuration in organic compounds by NMR spectroscopy and computational methods. Chem. Rev. 107, 3744–3779.

Bocca, A.L., Amaral, A.C., Teixeira, M.M., Sato, P.K., Shikanai-Yasuda, M.A., Soares Felipe, M.S., 2013. Paracoccidioidomycosis: eco-epidemiology taxonomy and clinical and therapeutic issues. Future Microbiol. 8, 1177–1191.

Castellani, A., 1967. Maintenance and cultivation of common pathogenic fungi in distilled water. J. Trop. M. Hyg. 42, 181–184.

Cicero, D.O., Barbato, G., Bazzo, R., 2001. Sensitivity enhancement of a two-dimensional experiment for the measurement of heteronuclear long-range coupling constants, by a new scheme of coherence selection by gradients. J. Magn. Reson. 148, 209–213.

Clinical Laboratory Standards Institute (CLSI), 2008. M27-Reference Method for Broth Dilution Antifungal Susceptibility Testing of Yeasts, Approved Standard, Third ed. Wayne, PA.

Cruz, R.C., Werneck, S.M.C., Oliveira, C.S., Santos, P.C., Soares, B.M., Santos, D.A., Cisalpino, P.S., 2012. Conditions for determining the minimal inhibitory concentration (MIC) of seven antifungal agents against Paracoccidioides brasiliensis by microdilution: influence of different media, incubation times and temperatures. J. Clin. Microbiol. 50, 3415–3819.

Ge, H.M., Peng, H., Guo, Z.K., Cui, J.T., Song, Y.C., Tan, R.X., 2010. Bioactive alkaloids from the plant endophytic fungus Aspergillus terreus. Planta Med. 76, 822–824.

Gonçalves, V.N., Cantrell, C.L., Wedge, D.E., Ferreira, M.C., Soares, M.A., Jacob, M.R., Oliveira, F.S., Galante, D., Rodrigues, F., Alves, T.M.A., Zani, C.L., Junior, P.A.S., Murta, S., Romanha, A.J., Barbosa, E.C., Kroon, E.G., Oliveira, J.G., Gomez-Silva, B., Galetovic, A., Rosa, C.A., Rosa, L.H., 2016. Fungi associated with rocks of the Atacama Desert: taxonomy, distribution, diversity, ecology and bioprospection for bioactive compounds. Environ. Microbiol. 18, 232–245.

Hochlowski, J.E., Mullally, M.M., Spanton, S.G., Whittern, D.N., Hill, P., McAlpine, J.B., 1993. 5-N-acetylardeemin, a novel heterocyclic compound which reverses multiple drug resistance in tumor cells II. Isolation and elucidation of the structure of 5-N-acetylardeemin and two congeners. J. Antibiot. 46, 380–386.

Kimura, Y., Nakajima, H., Hamasaki, T., 1989. Structure of rosellichalasin, a new metabolite produced by Rosellinia necatrix. Agric. Biol. Chem. 53, 1699–1701.

Lin, Z.J., Zhang, G.J., Zhu, T.J., Liu, R., Wei, H.J., Gu, Q.Q., 2009. Bioactive cytochalasins from Aspergillus flavipes, an endophytic fungus associated with the mangrove plant Acanthus ilicifolius. Helv. Chim. Acta 92, 1538–1544.

Liu, R., Gu, Q., Zhu, W., Cui, C., Fan, G., Fang, Y., Zhu, T., Liu, H., 2006. 10-Phenyl-[12]-cytochalasins Z7, Z8, and Z9 from the marine-derived fungus Spicaria elegans. J. Nat. Prod. 69, 871–875.

Liu, R., Lin, Z., Zhu, T., Fang, Y., Gu, Q., Zhu, W., 2008. Novel open-chain cytochalsins from the marine-derived fungus Spicaria elegans. J. Nat. Prod. 71, 1127–1132.

Matsumori, N., Kaneno, D., Murata, M., Nakamura, H., Tachibana, K., 1999. Stereochemical determination of acyclic structures based on carbon-proton spin-coupling constants a method of configuration analysis for natural products. J. Org. Chem. 64, 866–876.

Mendes, G., Gonçalves, V.N., Souza-Fagundes, E.M., Kohlhoff, M., Rosa, C.A., Zani, C. L., Cota, B.B., Rosa, L.H., Johann, S., 2016. Antifungal activity of extracts from Atacama Desert fungi against Paracoccidioides brasiliensis and identification of Aspergillus felis as a promising source of natural bioactive compounds. Mem. Inst. Oswaldo Cruz 111, 209–217.

Smith, W.B., Barfield, M., 1993. Letter to editor. Magn. Reson. Chem. 31, 696–697.

Sterflinger, K., Tesei, D., Zakharova, K., 2012. Fungi in hot and cold deserts with particular reference to microcolonial fungi. Fungal Ecol. 5, 453–462.

Wang, F.Z., Wei, H.J., Zhu, T.J., Li, D.H., Lin, Z.J., Gu, Q.Q., 2011. Three new cytochalasins from the marine-derived fungus Spicaria elegans KLA03 by supplementing the cultures with L- and D-tryptophan. Chem. Biodivers. 8, 887–894.

Xiao, L., Liu, H., Wu, N., Liu, M., Wei, J., Zhang, Y., Lin, X., 2013. Characterization of the high cytochalasin E and rosellichalasin producing-Aspergillus sp nov. F1 isolated from marine solar saltern in China. World J. Microbiol. Biotechnol. 29, 11–17.

Zhang, H.W., Zhang, J., Hu, S., Zhang, Z.J., Zhu, C.J., Ng, S.W., Tan, R.X., 2010. Ardeemins and cytochalasins from Aspergillus terreus residing in Artemisia annua. Planta Med. 76, 1616–1621.

Zhang, H.W., Ying, C., Tang, Y.F., 2014. Four ardeemin analogs from endophytic Aspergillus fumigatus SPS-02 and their reversal effects on multidrug-resistant tumor cells. Chem. Biodivers. 11, 85–91.

Zhang, H., Deng, Z., Guo, Z., Peng Yan Huang, N., He, H., Tu, X., Zou, K., 2015. Effect of culture conditions on metabolite production of Xylaria sp. Molecules 20, 7940–7950.